Journal of Extracellular Vesicles

RESEARCH ARTICLE OPEN ACCESS

Calibration of Flow Cytometers Enables Reproducible Measurements of Extracellular Vesicle Concentrations and Reference Range Establishment

Britta A. Bettin[1,2,3] | Bo Li[1,3,4] | Kim Falkena[5] | Ton G. van Leeuwen[2,3] | Christian Gollwitzer[6] | Zoltán Varga[7] | Nadine Ajzenberg[8,9] | Jovan P. Antovic[10,11] | Pascale Berckmans[12] | Edit I. Buzas[13,14,15] | Randy P. Carney[16] | Sean Cook[17] | Françoise Dignat-George[18,19] | Dorothee Faille[8,9] | Bernd Giebel[20] | Jennifer C. Jones[17] | Yohan Kim[21] | Romaric Lacroix[18,19] | Joanne Lannigan[22] | Fabrice Lucien[21,23] | Katariina Maaninka[24] | Erika G. Marques de Menezes[25,26] | Annette Meyer[27] | Rachel R. Mizenko[16] | Inge Nelissen[12] | John Nolan[28,29] | Philip J. Norris[25,26,30] | Desmond Pink[31,32] | Sumeet Poudel[33] | Stéphane Robert[34] | Pia R.-M. Siljander[24,35] | Vera A. Tang[36] | Tobias Tertel[20] | Tina Van Den Broeck[37] | Lili Wang[33] | Joshua A. Welsh[17,38] | Rienk Nieuwland[1,3] | Edwin van der Pol[1,2,3]

[1]Laboratory of Experimental Clinical Chemistry, Amsterdam UMC, Location University of Amsterdam, Amsterdam, The Netherlands | [2]Biomedical Engineering & Physics, Amsterdam UMC, Location University of Amsterdam, Amsterdam, The Netherlands | [3]Amsterdam Vesicle Center, Amsterdam UMC, Location University of Amsterdam, Amsterdam, The Netherlands | [4]Department of Laboratory Medicine, Nanfang Hospital, Southern Medical University, Guangzhou, Guangdong, China | [5]Exometry B.V., Amsterdam, The Netherlands | [6]Physikalisch-Technische Bundesanstalt (PTB), Berlin, Germany | [7]HUN-REN Research Centre for Natural Sciences, Magyar tudósok körútja 2., H-1117 Budapest, Hungary and Department of Physical Chemistry and Materials Science, Faculty of Chemical Technology and Biotechnology, Budapest University of Technology and Economics, Budapest, Hungary | [8]Université Paris Cité, INSERM U1148, LVTS, Paris, France | [9]Laboratoire d'Hématologie, AP-HP, Hôpital Bichat, Paris, France | [10]Coagulation, Clinical Chemistry, Karolinska University Hospital, Stockholm, Sweden | [11]Department of Molecular Medicine & Surgery, Karolinska Institutet, Stockholm, Sweden | [12]Environmental Intelligence Unit, Flemish Institute for Technological Research, Mol, Belgium | [13]Department of Genetics, Cell- and Immunobiology, Semmelweis University, Budapest, Hungary | [14]HCEMM-SU Extracellular Vesicle Research Group, Semmelweis University, Budapest, Hungary | [15]HUN-REN-SU Translational Extracellular Vesicle Research Group, Semmelweis University, Budapest, Hungary | [16]Department of Biomedical Engineering, University of California, Davis, California, USA | [17]Translational Nanobiology Section, Laboratory of Pathology, Center for Cancer Research, National Cancer Institutes, National Institutes of Health, Bethesda, Maryland, USA | [18]Aix Marseille Univ, INSERM 1263, INRAe 1260, C2VN, Marseille, France | [19]Department of Hematology, Biogenopole, CHU La Timone, APHM, Marseille, France | [20]Institute for Transfusion Medicine, University Hospital Essen, University of Duisburg-Essen, Essen, Germany | [21]Department of Urology, Mayo Clinic, Rochester, Minnesota, USA | [22]Flow Cytometry Support Services, LLC, USA | [23]Department of Immunology, Mayo Clinic, Rochester, Minnesota, USA | [24]EV group and EV core, Molecular and Integrative Biosciences Research Programme, Faculty of Biological and Environmental Sciences, University of Helsinki, Helsinki, Finland | [25]Vitalant Research Institute, San Francisco, California, USA | [26]Department of Laboratory Medicine, University of California, San Francisco, California, USA | [27]European Center for Single Cell Solutions ESS, BD Biosciences, Heidelberg, Germany | [28]Scintillon Institute, San Diego, California, USA | [29]Cellarcus Biosciences, La Jolla, California, USA | [30]Department of Medicine, University of California, San Francisco, California, USA | [31]Nanostics Inc. Edmonton, Alberta, Canada | [32]Vivian Triana, Nanostics Inc, Edmonton, Alberta, Canada | [33]Biosystems and Biomaterials Division, National Institute of Standards and Technology, Gaithersburg, Maryland, USA | [34]Aix Marseille Univ, INSERM 1263, INRAe 1260, C2VN, AMUTICYT Core Facility, Marseille, France | [35]Finnish Red Cross Blood Service, Helsinki, Finland | [36]University of Ottawa Flow Cytometry & Virometry Core Facility, Faculty of Medicine, Ottawa, Canada | [37]Medical and Scientific Affairs, BD Biosciences, Erembodegem, Belgium | [38]Advanced Technology Group, BD Biosciences, San Jose, California, USA

Correspondence: Britta A. Bettin (b.a.bettin@amsterdamumc.nl)

Received: 1 May 2025 | **Revised:** 11 September 2025 | **Accepted:** 8 October 2025

Keywords: blood plasma | calibration | extracellular vesicles | flow cytometry | reference ranges | reproducibility | standardization

Rienk Nieuwland and Edwin van der Pol share senior authorship.

ABSTRACT

The concentration of cells is a key component of modern blood tests. Given the biomarker potential of extracellular vesicles (EVs) in blood, we aimed to establish reference ranges for blood cell-derived EVs using flow cytometry. To address the orders-of-magnitude variability in reported EV concentrations between different flow cytometers (FCMs), we first validated a calibration methodology to enable reproducible EV concentration measurements. The methodology was evaluated in an interlaboratory comparison study and shows that calibration reduces the median absolute deviation of EV concentrations measured on 25 different FCMs from 67 % to 25 %–31 %. The calibration methodology was then used to determine reference ranges of erythrocyte-, leukocyte-, and platelet-derived EVs in human blood plasma in a cohort of healthy individuals ($n = 224$). This study demonstrates that calibration enables comparable concentration measurements of blood cell-derived EVs, thereby bringing EVs one step closer to clinical applications.

1 | Introduction

Extracellular vesicles (EVs), including exosomes, are submicrometer particles released by cells into body fluids, such as blood and urine (Welsh et al. 2024; Caby et al. 2005; Raj et al. 2012; Chatterjee et al. 2024). EVs have gained increasing attention for their diagnostic and therapeutic potential in cancer and cardiovascular disease, both among the leading causes of mortality (Li et al. 2009; Loyer et al. 2014; World Health Organization; Bray et al. 2021; Enciso-Martinez et al. 2025). This interest in EVs is reflected by the annual market size of EV technologies, which is expected to exceed $3 billion within the next decade (Exosomes Market Size, and Share—Trends Analysis Report 2032). Nevertheless, in contrast to the well-established concentration of cells in blood, the concentration of EVs in blood lacks consensus, despite decades of research. Currently, no method can reliably measure the concentrations of (blood) cell-derived EVs (Abbott 2023; Exosome Technologies Market Size, Share & Forecast - 2031), which undermines the potential of EV-based diagnostic and therapeutic applications.

The goal of EV-based diagnostics is to relate properties of EVs, such as their biochemical composition, concentration, or function, to the health status of an individual. Although EVs have shown diagnostic potential (Nanou et al. 2018; Berezin et al. 2015; Logozzi et al. 2009; Fais et al. 2016; Hoshino et al. 2020), findings are often irreproducible because data are reported in arbitrary units, which are meaningful only within a single laboratory. For comparison, the concentrations of well-established clinical parameters, such as blood cells and analytes like cholesterol, glucose, and haemoglobin, are regulated by International Organization for Standardization (ISO) standards, and therefore measured in SI-units with uncertainties of 3 %–15 % [e.g., cholesterol: 10 % (2025 CLIA Acceptance Limits for Proficiency Testing—Westgard QC), glucose: 15 % (International Organization for Standardization 2013), haemoglobin: 3.3 % (Vis and Huisman 2016)]. Consequently, these parameters can be reliably compared across clinical laboratories, making them essential for standardized diagnostics. To achieve similar clinical utility for EV-based diagnostics, standardization for EV concentration measurements is a prerequisite.

Regarding therapeutic applications, the functional activity of EVs is influenced by their concentration, amongst other factors. Regulatory agencies, such as the European Medicines Agency (EMA) and US Food and Drug Administration (FDA) require reliable determinations of the concentrations of active agents and consequently therapeutic applications of EVs should require reliable measurements of EV concentrations.

Thus, EV-based diagnostics and therapeutics require reproducible measurements of EV concentrations, which can be accomplished with flow cytometry. A flow cytometer (FCM) is designed to measure fluorescence and light scattering signals of single cells in a fluid stream at a rate of thousands per second (Welsh et al. 2023). Due to the high throughput, flow cytometry can provide statistically robust information about fluorescently-stained EV populations present in body and biofluids (van der Pol et al. 2022). Moreover, FCMs can determine the concentration and diameter more accurately and precisely than most other techniques (van der Pol et al. 2022; van der Pol et al. 2014). Importantly, FCMs are widely available in clinical laboratories and hospitals, which supports their potential for clinical translation. Measuring EV concentrations with an FCM is, however, complicated due to (1) the complexity of EV-containing samples, (2) the physical properties of EVs, (3) differences between FCM hardware, and (4) data in arbitrary units. In addition, EV concentrations are affected by biospecimen factors and pre-analytical variables, including blood collection, processing, and storage (Welsh et al. 2024; Lucien et al. 2023).

First, body fluids are complex and also contain particles other than EVs (Tian et al. 2020; Van Herwijnen et al. 2016), like lipoprotein particles in blood plasma (Sódar et al. 2016), which can lead to misidentification of EVs. Second, EVs are so small and heterogenous in size and composition that FCMs are unable to detect all EVs (van der Pol et al. 2014; van der Pol et al. 2018; Arraud et al. 2014; de Rond et al. 2018). As a result, FCMs detect only the fraction of EVs whose fluorescence and light scattering signals exceed the lower limit of detection (LoD). Throughout this manuscript, the term "EV concentration" therefore refers to the concentration of detectable EVs. Third, the LoDs of FCMs differ due to differences in hardware. As the LoD determines the fraction of detectable EVs, the FCM hardware impacts the measured EV concentration (Welsh et al. 2023; Robert et al. 2009; Bettin et al. 2023). Fourth, the detected signals have arbitrary units, which precludes reporting measured EV concentrations within well-defined signal ranges. Hitherto, these four complications together have made it difficult to report comparable EV concentrations (Welsh et al. 2023; van der Pol et al. 2018).

To obtain reliable and comparable EV concentration measurements using flow cytometry, standardization is essential. Standardization involves calibrating the flow rate, fluorescence

signals, and light scattering signals (Welsh et al. 2023, 2021). Calibration relates measured signals in arbitrary units to standard units using reference materials (RMs) (Welsh et al. 2023; Bettin et al. 2023). Once calibrated, EV concentrations can be reported within well-defined fluorescence and size ranges and can be compared across FCMs and laboratories.

Over the years, several attempts have been made to standardize EV concentration measurements (van der Pol et al. 2018; Robert et al. 2009; Lacroix et al. 2010; Cointe et al. 2017; Chandler et al. 2011; Welsh, Jones, et al. 2020). However, these studies were often limited, either involving only a small number of FCMs, utilizing no or only partial signal calibration, or lacking ready-to-measure biological test samples.

Here, we combined, refined, and validated previously published methods (van der Pol et al. 2018; Welsh, Jones, et al. 2020; de Rond et al. 2018; van der Pol et al. 2012; Doornbos et al. 1994; Vogt et al. 1989) to measure reliable and comparable EV concentrations. The resulting methodology is based on RMs, quality control (QC) materials, a ready-to-measure EV-containing biological test sample, and procedures to calibrate FCMs. We evaluated the methodology in the largest global interlaboratory EV comparison study to date, including 25 FCMs from 18 different laboratories. To demonstrate the clinical applicability of the validated methodology, we determined reference ranges of blood cell-derived EV concentrations, within well-defined fluorescence and size ranges, in blood plasma from 224 healthy humans.

2 | Materials and Methods

2.1 | Study Design and Participants

The aim of the study was to (1) validate a methodology that allows improving the comparability of measured EV concentrations by calibrating the flow rate, fluorescence signals, and light scattering signals of an FCM and (2) demonstrate the applicability of the methodology by establishing reference ranges of EVs in human blood plasma. Figure 1 shows an overview of the methodology.

The methodology was tested in a global interlaboratory comparison study. All participants had a publication track record on EV detection by flow cytometry and were asked to have at least one FCM capable of (1) differentiating 125 nm polystyrene beads from 100 nm polystyrene beads or background noise by light scattering, (2) detecting allophycocyanin (APC) and phycoerythrin (PE) fluorescence, (3) measuring EVs directly in diluted blood plasma at high throughput (>1000 events/second). Initially, 38 FCMs from 24 different laboratories enrolled. Data were submitted for 26 FCMs from 19 laboratories, while no data were submitted for 12 FCMs. Of these, one FCM did not meet criterion (1), leaving the evaluation of the methodology to be conducted on 25 FCMs from 18 laboratories (Table 1). Data processing was performed by the coordinating laboratory, following common practice in interlaboratory comparison studies to enhance data comparability and minimize confounding technical variation.

The reference ranges were established by measuring blood cell-derived EV concentrations in blood plasma from 224 healthy volunteers with a calibrated FCM in one laboratory.

2.2 | Samples and Sample Distribution

Buffers, RMs, QC materials, and a ready-to-measure human plasma EV test sample (PEVTES) together with a protocol were disseminated to the participating laboratories (Supporting Information 1). RMs were used to calibrate the flow rate, fluorescence signals, and light scattering signals, and QC materials to validate instrument stability. Additionally, a webinar (https://www.metves.eu/output/videos) was conducted to provide detailed information about the protocol.

2.3 | Assessment of Instrument Sensitivity

All participants measured Rosetta Calibration bead mix (CAL003, Exometry B.V.) according to the instructions of the manufacturer (Supporting Information 1) and sent the data files to the coordinating laboratory. Rosetta Calibration bead mix contains polystyrene beads with traceably measured mean diameters between 70 and 994 nm. Files were analysed with Rosetta Calibration Software (Exometry B.V.) to determine whether the FCM was able to differentiate a scatter signal of 125 nm polystyrene beads from either the 100 nm polystyrene beads or the background noise. In case the scatter signal of 125 nm polystyrene beads could not be resolved; participants were asked to change the measurement settings to improve sensitivity. Participants who succeeded to meet the aforementioned criterion continued to perform measurements of all samples (RMs, QC samples and PEVTES) according to the protocol (Supporting Information 1).

2.4 | Calibration

Flow rate, fluorescence and light scattering calibrations were performed on the same day as the measurements of all other samples.

2.4.1 | Flow Rate Calibration

The flow rate was calibrated by measuring the counts of RMs and QC materials according to the following four steps.

First, we developed and assigned a metrologically traceable concentration to solid silica nanoparticles (SNP). SNP (ID: SNP 083) were developed by the Biological Nanochemistry Research Group, Institute of Materials and Environmental Chemistry, Research Centre for Natural Sciences, Budapest, Hungary. The number concentration of SNP was traceably determined by small-angle x-ray scattering (SAXS) at the Physikalisch-Technische Bundesanstalt, Berlin, Germany and single particle inductively coupled plasma mass spectrometry (spICPMS) at the National Measurement Laboratory, LGC Limited, Teddington, United Kingdom (Schürmann et al. 2024).

Second, SNPs were used to assign concentrations to QC materials (Peak 3 of vCal Nanorainbow Beads, Cellarcus Biosciences; 200 nm polystyrene beads of Rosetta Calibration beads, CAL003, Exometry B.V.). SNP and QC materials were diluted and measured (Aurora, Cytek Biosciences) according to the protocol (Supporting Information 1). To analyse the flow rate, the measured

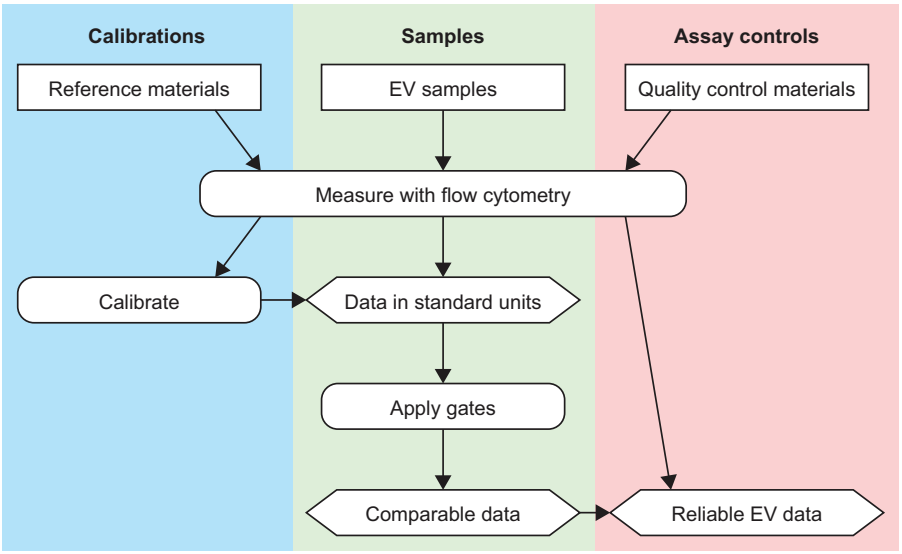

FIGURE 1 | Calibration methodology workflow. Schematic workflow for obtaining comparable and reliable extracellular vesicle (EV) concentrations using flow cytometry. The process integrates calibration (blue), sample measurements (green) and assay controls (red). Reference materials (calibrants) convert arbitrary fluorescence signals and light scattering signals into standard units. In this study, calibration is also used to determine the lower limit of detection (LoD) of the fluorescence and light scattering detectors of each flow cytometer (FCM). Assay controls, such as buffer-only controls or buffer with reagent controls are needed to confirm that detected signals originate from EVs. Combining calibrated data with assay controls ensures standardized and reproducible and EV measurements, supporting both research and clinical applications.

sample volume V was determined according to:

$$V\,[\mu\mathrm{L}] = \frac{P_{SNP}}{C_{\mathrm{SNP}}\,[\mu\mathrm{L}^{-1}]} \tag{1}$$

where P is the number of counted particles and C_{SNP} is the specified concentration of the SNP after dilution. Throughout this manuscript, the units in equations are indicated between brackets. Next, the flow rate Q of the FCM was determined by:

$$Q\,[\mu\mathrm{L}/\,\mathrm{min}] = \frac{V\ [\mu\mathrm{L}]}{\mathrm{t}\,[\mathrm{min}]} \tag{2}$$

where t is the acquisition time of the sample. Particle concentrations were assigned to the QC samples by:

$$C_{QC}\,\left[\mu\mathrm{L}^{-1}\right] = \frac{P_{QC}}{Q\ [\mu\mathrm{L}/\,\mathrm{min}]\ \mathrm{t}\ [\mathrm{min}]} \tag{3}$$

During this procedure, the flow rate based on SNP deviated <0.5 % from the flow rate determined by the flow rate sensor, and the CV of the flow rate was <3.8 %.

Third, SNPs and QC materials were diluted and measured on each FCM according to the protocol (Supporting Information 1), and the flow rates were calculated according to Equations (1) and (2).

Fourth, the flow rate used to calibrate the PEVTES measurement was selected based on SNPs or QC materials (Peak 3of vCal Nanorainbow Beads, Cellarcus Biosciences; 200 nm polystyrene beads of Rosetta Calibration beads, CAL003, Exometry B.V.), depending on the variation of the flow rate between consecutive measurements. To quantify this variation, we calculated the MAD of the determined flow rates for each FCM (Table 1). If the flow rate variation was <20 % MAD and the flow rate based on SNP was within 20 % of the median flow rate of all beads, the SNP-based flow rate was selected for further analysis (nine FCMs). If the SNP-based flow rate did not meet these criteria, but the flow rate variation based on QC materials was <20 % MAD, we selected the median flow rate of the QC materials, assuming the SNP measurement was faulty (13 FCMs). If neither the flow rate variation based on all beads nor the flow rate variation based on QC materials was <20 % MAD, the flow cytometer was excluded from further analysis (three FCMs).

For the reference range study, ApoCal Mix beads (1524, Apogee Flow Systems) were used to validate the flow rate of a calibrated syringe pump, because SNPs were not yet available.

2.4.2 | Fluorescence Calibration

Fluorescence calibration was performed for each FCM with custom-made dried 2-µm APC and PE MESF beads (R&D Lot# 2364–87, 2364–89, BD Biosciences). MESF beads were diluted and measured according to the protocol (Supporting Information 1). Data and specified MESF values were logarithmically transformed and fitted by linear regression to relate the arbitrary units of fluorescence to standard units. The slope a and intercept b of the linear regression are used to relate the arbitrary units (a.u.) of the fluorescence intensity I to MESF units as follows:

$$I\,[\mathrm{MESF}] = 10^{a\cdot\log_{10}I[\mathrm{a.u.}]+b} \tag{4}$$

Figure 2A shows a representative example of a fluorescence calibration for the APC and PE detectors of an FCM (Northern Lights, Cytek Biosciences). The fluorescence calibration of each FCM can be found in Supporting Information 2.

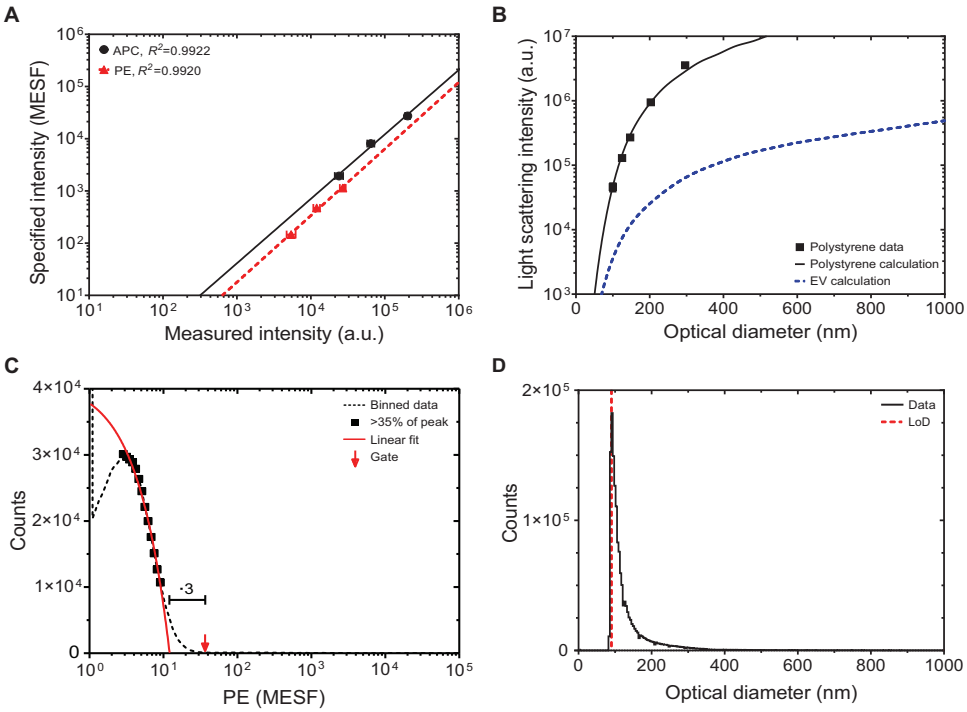

FIGURE 2 | Example of fluorescence and light scattering calibrations and determination of the lower limit of detection (LoD) of a flow cytometer (FCM; Northern Lights, Cytek Biosciences). (A) Calibration of the allophycocyanin (APC; solid black line) and phycoerythrin (PE; dashed red line) detectors of an FCM. The measured arbitrary units (a.u.) are related to the specified number of molecules of equivalent soluble fluorochrome (MESF) of custom-made reference particles using a linear regression. Error bars indicate the standard deviation. (B) Light scattering calibration (Rosetta Calibration) of the side scattering detector of the same FCM as in panel A. Measured (symbols) and calculated (lines) light scattering intensities of polystyrene beads (black solid line) and EVs (blue dashed line). Shown are the measured light scattering intensity in a.u. versus the optical diameter polystyrene beads in nm. Polystyrene beads were modelled as solid spheres with a refractive index (RI) of 1.63 at an illumination wavelength of 405 nm. EVs were modelled as core-shell particles with a shell thickness of 6 nm, a shell RI of 1.48 and a core RI of 1.38. (C) The LoD (and gate) of the fluorescence detector (red arrow) was determined by making a histogram of the fluorescence intensities on a logarithmic scale with 24 bins per decade (black dashed line). Values right from the peak and exceeding 35 % of the peak amplitude (square symbols) are fitted with a linear function (red solid line). The LoD is defined as the intersection of the linear fit with the horizontal-axis multiplied with 3. Fluorescent LoDs (and gates) were determined based on 30-fold diluted plasma EV test sample (PEVTES). (D) The LoD of the light scattering detector (red dashed line), expressed in terms of optical diameter of EVs in nm, is defined as the mode of the optical diameter distribution of the 30-fold diluted plasma EV test sample under the assumption of the thickness and core/shell structure of EVs. The bin width is 1 nm.

To determine the reference range of EVs from healthy volunteers, fluorescence calibration of the APC, BV, and PE detectors of an FCM were performed by cross-calibration of rainbow beads (SPHERO Rainbow calibration particles, eight peaks, 3.0–3.4 µm, lot EAM02, Spherotech Inc) with custom-made molecules of equivalent soluble fluorochrome (MESF) beads, specifically 2 µm APC quantification beads (lot 2364-175, custom-order, BD Biosciences), 3 µm BV421 quantification beads (lot MM2337-25, custom-order, BD Biosciences), and SPHERO Calibration Particles PE [catalogue number ECFP-F2-5K, lot AK01, Spherotech Inc, Supporting Information 3, (MIFlowCyt-EV)].

2.4.3 | Light Scattering Calibration

Light scattering signals were calibrated using Rosetta Calibration bead mix (CAL003, Exometry B.V.) that was diluted according to the instructions of the manufacturer (Supporting Information 1) and measured at the same settings as EVs. The calibration was performed with Rosetta Calibration Software (Exometry B.V.), which utilizes Mie theory to relate light scattering signals to the optical diameter of a particle. Polystyrene beads were modelled as solid spheres with a refractive index (RI) obtained from the dispersion relation as published by Kasarova et al. at 20°C (Kasarova et al. 2007). Dispersion relations were used to account for differences in the illumination wavelength between FCMs. For water, the suspension fluid of beads, the dispersion relation as published by Daimon et al. at 20°C was used (Daimon and Masumura 2007). For Dulbecco's phosphate buffered saline (DPBS), the suspension fluid for PEVTES, the dispersion relation of water plus 0.002 was used. To model EVs, a shell thickness of 6 nm, a shell RI of 1.48, and a core RI of 1.38 were assumed (van der Pol et al. 2021). Figure 2B shows a representative example of a light scattering calibration for an FCM (Northern Lights, Cytek Biosciences). All details of the model were published elsewhere (de Rond et al. 2018) and the model has been validated in an earlier interlaboratory comparison study (van der Pol et al. 2018). The light scattering calibration of each FCM can be found in Information 4. Light scattering intensities were related to optical diameters, which were calculated with a step size of 10 nm, by linear interpolation.

2.5 | Data Acquisition

Laboratories were instructed to trigger on their most sensitive scatter detector but set the flow rate, detector voltage, laser powers, time interval after maintenance, and trigger threshold according to their own judgement. The performance of an FCM in this study does therefore not reflect the generic performance of a brand or type of FCM.

2.5.1 | Measuring of the Plasma EV Test Sample (PEVTES)

An in-house developed plasma EV test sample (PEVTES), prepared from human blood plasma, was used as a ready-to-measure, EV-containing sample, that resembles subcellular particles in plasma. Details on the preparation of PEVTES can be found elsewhere (Bettin et al. 2023) (Supporting Information 4). Briefly, Plasma EVs were stained with antibodies against cell-type-specific proteins. For the interlaboratory comparison study, PEVTES was double-stained with CD235a-PE (R7078; JC159; f.c., 25 µg/mL; Dako) for erythrocyte-derived EVs and CD61-APC (17-0619-42; VI-PL2; final concentration (f.c.), 8.33 µg/mL; eBioscience) for platelet-derived EVs. Next, to separate EVs from unbound dye, soluble proteins, and reduce lipoprotein particles, size-exclusion chromatography (SEC) was performed (qEVsingle/70 nm 1004125; Izon Science). To remove remaining platelets from plasma, plasma was filtered using a 0.8-µm pore-size polycarbonate membrane filter (ATTP02500, Isopore, Merck Millipore). To stabilize the SEC-isolated EVs, a buffer of 1 M D-(+)-trehalose dihydrate (T9531, Sigma Aldrich, f.c. 0.5 M) and 5 % bovine serum albumin (A9647, Sigma Aldrich, f.c. 0.5 %;) was added (Robert et al. 2009; Bettin et al. 2023). PEVTES was shipped on dry ice to the participating laboratories and measured according to the provided protocol (Supporting Information 1). To avoid swarm detection (van der Pol et al. 2012, Buntsma et al. 2023), a serial dilution was performed (Supporting Information 1), and the results of the swarm detection analysis are shown in Supporting Information 2. No swarm detection was observed in the 30-fold diluted PEVTES across participating FCMs. Therefore, 30-fold diluted PEVTES was used for further analysis.

2.5.2 | Reference Ranges of Blood Cell-Derived EV Concentrations in Human Blood Plasma

To establish the reference ranges of blood cell-derived EV concentrations in human blood plasma, blood from 224 healthy volunteers was collected. Collection of blood was performed according to the guidelines of the medical ethical committee of the Academic Medical Centre, University of Amsterdam (W19_271#19.421). All donors denied having a disease, use drugs and/or medication, and were screened for hepatitis B, hepatitis C, and human immunodeficiency virus (HIV). Venous blood was collected using a 21-gauge needle (368607, BD Biosciences), and the first 3.5 mL of blood was discarded. One tube of Ethylenediaminetetraacetic acid (EDTA) blood (Buntsma et al. 2022) of 6 mL (367899, BD Biosciences) was collected from each donor and plasma was prepared by double centrifugation. Blood was centrifuged at 2500 × *g* for 15 minutes at 20°C, acceleration speed 9, and deceleration speed 1 using a Rotina 380 R equipped with a swing-out rotor and radius of 155 mm (Hettich Zentrifugen). Plasma was collected 10 mm above the buffy coat (determined with a Lego brick) using a plastic Pasteur pipette (86.1171.001, SARSTEDT) and transferred into a new 15-mL polypropylene centrifuge tube (62.9924272, SARSTEDT). Subsequently, the plasma was centrifuged at the same settings used for whole blood. Afterward, plasma was collected to 10 mm above the pellet to reduce platelet contamination and transferred into a new 15-mL tube. Next, 100 µL plasma was aliquoted into cryogenic vials (72.692.005, SARSTEDT) frozen in liquid nitrogen for 15 minutes, and stored at −80°C until analysis.

The concentration of erythrocyte-derived EVs (CD235a-PE), leukocyte-derived EVs (CD45-APC), and platelet-derived EVs (CD61-BV421) were measured in freeze-thawed plasma with one calibrated FCM (Apogee A60-Micro, Apogee Flow Systems). A detailed description of the analysis can be found in the MIFlowCyt-EV (Welsh et al. 2021) and the MIBlood-EV (Lucien et al. 2023) (Supporting Informations 3 and 5).

3 | Data Analysis

3.1 | Signal Processing

3.1.1 | Area or Height Parameter

For fluorescence and light scattering signals close to the background noise, the height parameter is biased toward the mode of each pulse, potentially resulting in a detectable offset. Therefore, the pulse area is the preferred parameter. However, we observed that for eight detectors in this study, the area parameter was less precise than the height parameter. To mitigate the impact of this imprecision on the results, the area parameter was used for most detectors (64 detectors), unless (1) the CV of a bead population determined using the area parameter was 3 % higher than that determined using the height parameter (eight detectors), or (2) the area parameter was unavailable (three detectors). To determine the CV for (1) the APC and PE detectors, the third bead population of vCal Nanorainbow Beads (cat. CBS6-1000, lot. 20911, Cellarcus Biosciences) was used, and (2) the light scattering detector, the 150-nm fluorescent polystyrene bead in the Rosetta Calibration bead mix (CAL003, Exometry B.V.) was used.

3.1.2 | Signal Processing for Uncalibrated Data

For uncalibrated data (Figure 3), the concentration of erythrocyte-derived and platelet-derived EVs in PEVTES was calculated as described in Section 3.3, 'EV Number Concentration'.

3.1.2.1 | Flow Rate. For uncalibrated data (Figure 3), the flow rate indicated by the acquisition software was used to calculate EV concentrations.

3.1.2.2 | Gate Determination. For uncalibrated data (Figure 3), the fluorescence gates that differentiate fluorescent-positive counts from background noise were determined individually for each FCM using a published script (MATLAB R2020b, MathWorks) (Gankema et al. 2022). The approach is

outlined in Section 3.2.1.1, 'Limit of Detection of Fluorescence Detectors'. The gates were applied to data in arbitrary units. No gate was applied to the light scattering signal.

3.2 | Signal Processing for Calibrated Data

3.2.1 | Limit of Detection

In technical terms, the LoD of an optical detector is the lowest amplitude at which the signal is distinguishable from the background noise at a defined confidence level. For both fluorescence and light scattering detectors, we developed and applied procedures to determine LoDs that are both practical and insightful in the context of EV flow cytometry.

3.2.1.1 | Limit of Detection of Fluorescence Detectors. We defined the LoD of the fluorescence detectors as the fluorescent gates, which are normally applied to differentiate fluorescently stained particles from the background noise. Fluorescent gates were determined based on 30-fold diluted PEVTES and a published script (MATLAB R2020b, Mathworks) (Gankema et al. 2022). Figure 2C shows how fluorescence gate determination was automated. In short, a histogram of the measured fluorescence intensities, expressed in units of MESF is created on a logarithmic scale with 24 bins per decade. Values right from the peak and exceeding 35 % of the peak amplitude are fitted with a linear function. The intersection of the linear fit with the horizontal-axis multiplied with 3 is used as the fluorescent gate.

3.2.1.2 | Limit of Detection of the Optical Diameter. The LoD of the light scattering detectors, expressed in terms of the optical diameter of EVs in nm, was defined as the mode of the optical diameter distribution (bin width = 1 nm) of the 30-fold diluted PEVTES (Figure 2D). Although the mode diameter is directly affected by the trigger threshold, we deliberately did not use the trigger threshold to estimate the LoD, because (1) for FCMs from Apogee Flow Systems the units differ between the data acquisition software and the fcs file, thereby precluding a reliable read-out of the LoD based on the adjusted trigger threshold, and (2) not all FCMs have a trigger threshold that results in an infinite response function (see Data availability).

3.2.2 | Gate Determination for Calibrated Data

To compare the concentrations of cell-type-specific EVs, two different groups were formed based on the established LoDs of all FCMs able to detect 125 nm polystyrene beads (Figure 4).

Group 1 includes all FCMs with LoDs lower than the median LoDs for both the calibrated fluorescence detectors and optical diameters (nm). The group boundaries for group 1 are set at 103 MESF APC, 16 MESF PE, and 146 nm. Next, we applied gates to both groups, with the gates set to equal the least sensitive FCMs within each group (Supporting Information 6). Consequently, the gates for group 1 are 16 MESF PE and 133 nm for erythrocyte-derived EVs, while for platelet-derived EVs, the gates for group 1 are set at 98 MESF APC and 113 nm.

Group 2 includes all FCMs with LoDs lower than the 95th percentile of LoDs for both the calibrated fluorescence detectors and optical diameters (nm). The boundaries of group 2 are set at 415 MESF APC, 77 MESF PE and 242 nm for both EV subtypes. The gates applied to group 2 are 396 MESF APC, 77 MESF PE and 242 nm for both EV types. FCMs that did not fall within 95th percentile of the LoD of calibrated fluorescence detectors and optical diameters were considered unrepresentatively insensitive and were therefore excluded from further analysis.

3.3 | EV Number Concentration

The EV concentration in the PEVTES is defined as the number of EVs per volume of the undiluted PEVTES sample. EV concentrations were determined as follows:

$$C_{\mathrm{EV}}\left[\mathrm{mL}^{-1}\right] = \frac{E \cdot d \cdot 1{,}000}{Q\,[\mu\mathrm{L}/\,\mathrm{min}] \cdot t\,[\mathrm{min}]} \tag{5}$$

where E are the number of fluorescent-positive counts in the given gate, d is the dilution factor, and Q and t were defined as previously described.

3.4 | Reference Ranges of Blood Cell-Derived EV Concentrations for Human Blood Plasma

To establish the reference ranges, outliers were first identified and discarded using the Tukey method. Briefly, the lower and upper cutoffs for outliers were defined as Q1 − [1.5 × interquartile range (IQR)] and Q3 + (1.5 × IQR), respectively, where Q1 is the lower sample quartile, Q3 is the upper sample quartile and IQR = Q3–Q1 (Horn and Pesce 2003). Afterward, EV concentration reference ranges were calculated as described in Section .3.3 'EV Number Concentration' and are expressed between the 2.5th percentile and 97.5th percentile.

A detailed description of the analysis can be found in the MIFlowCyt-EV (Supporting Information 3).

3.5 | Software and Statistics

Flow cytometry data were processed using FlowJo (v 10.7.1, FlowJo) and custom-build software (MATLAB R2020b, MathWorks) to automate data calibration and data processing.

Statistical analyses were performed using Prism 8.0 (GraphPad). Graphs were made with Prism 8.0 (GraphPad) and Adobe Illustrator (V 26.2.1, Adobe Inc). The MAD and the COR were calculated as measures of variation. The MAD is calculated as follows:

$$MAD = \frac{median\left(\forall c_i \in \vec{c}, |c_i - median\left(\vec{c}\right)|\right)}{median\left(\vec{c}\right)} \cdot 100\% \tag{6}$$

where $\vec{c}$ represents a vector of measured particle concentrations with elements c_i, $\forall$ and $\in$ are mathematical operators meaning "for all" and "element of", respectively, and *median* is a statistical measure that represents the middle value of a dataset when it is sorted in ascending order. If the dataset has an odd number of

elements, the median is the middle value. If the dataset has an even number of elements, the median is the average of the two middle values. The MAD was selected as a statistical measure to quantify the variation of measured concentrations, because it is applicable to skewed datasets and it takes all datapoints into account without being sensitive to outliers, in contrast to, for example, the coefficient of variation.

The COR is calculated as follows:

$$COR = \frac{x_m - x_o}{x_m + x_o} \cdot 100\% \quad (7)$$

where x_m is the maximum value and x_o the minimum value in the dataset.

Data Availability

Study part	Figures	Link
Interlaboratory comparison study, evaluation of the calibration methodology	2–5	https://figshare.com/s/9a847bd8ede732ba9c1e
Reference ranges of EV concentrations	6	https://figshare.com/s/60590e618d96cc1374f8

4 | Results

4.1 | Selection of flow cytometers

Thirty-eight FCMs from 24 laboratories enrolled in the study. We received data from 26 FCMs from 19 laboratories. FCMs were included or excluded based on calibration and QC outcomes (Table 1). One FCM was unable to differentiate 125 nm polystyrene beads from 100 nm polystyrene beads and was therefore excluded. Additionally, for the APC and PE detector, two and one FCM(s) were excluded, respectively, because the fluorescence calibration did not result in a linear fit ($R^2 > 0.98$). Three additional FCMs were excluded because the flow rate could not be established during the PEVTES measurement, as discussed in the Materials and Methods. The remaining 20 FCMs for APC and 21 FCMs for PE were split into two sensitivity-based groups (as discussed in Figure 4 and the Materials and Methods). FCMs that did not fall within the 95th percentile of the LoD of calibrated fluorescence detectors and optical diameters were excluded as unrepresentatively insensitive, leaving 18 FCMs for APC and 19 FCMs for PE. For these instruments, EV concentrations were determined when ≥20 fluorescent-positive counts were detected. Group 1 contains 8 FCMs for PE and seven FCMs for APC, while group 2 contains 19 FCMs for PE and 18 FCMs for APC. Table 1 provides an overview of the included and excluded FCMs.

4.2 | EV Concentrations Without Calibration

We aim to validate a methodology that allows for comparing EV concentrations in a global interlaboratory comparison study. All laboratories measured the same PEVTES, which contains erythrocyte and platelet-derived EVs stained with CD (cluster of differentiation) 235a-PE and CD61-APC, respectively. In this manuscript, we refer to EVs as erythrocyte-derived EVs or platelet-derived EVs based on positive staining with CD235a-PE or CD61-APC, respectively. For comparison, we first assessed the measured EV concentrations in PEVTES without calibration. Figure 3 shows that the concentrations of EVs exceeding the FCM-specific trigger threshold and background fluorescence intensities span about two orders of magnitude for both EV types, when compared LoDs are not accounted for.

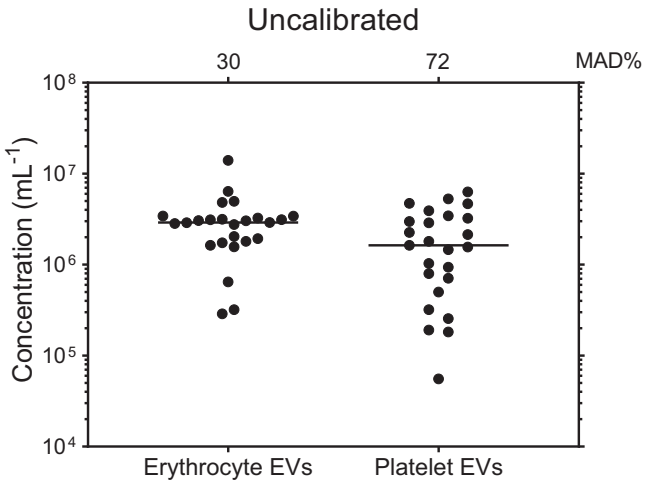

FIGURE 3 | Concentration of erythrocyte-derived [cluster of differentiation (CD) 235a-phycoerythrin (PE)] and platelet-derived [CD61-allophycocyanin (APC)] extracellular vesicles (EVs) in a 30-fold diluted plasma EV test sample (PEVTES) measured (symbols) with flow cytometers participating in an interlaboratory comparison study without calibration. Black lines indicate the median concentration measured on 25 different flow cytometers in different laboratories. The variation of the measured concentrations was quantified using the median absolute deviation (MAD).

To describe the variation of the EV concentrations statistically, we calculated the median absolute deviation (MAD), which is the relative distance of all datapoints to the median. In contrast to the coefficient of variation (CV), the MAD (1) takes all datapoints into account, (2) is insensitive to outliers, and (3) is applicable to skewed datasets. The MAD for the concentration of erythrocyte-derived and platelet-derived EVs was 30 % and 72 %, respectively. An analysis of the coefficient of range (COR) can be found in Figure S7.1 (Supporting Information 7).

4.3 | Detection Limits in Standard Units by Calibration

To allow data comparison between different FCMs, EV concentrations need to be determined within the same fluorescence and light scattering signal ranges. As these signals are scaled arbitrarily, the first step is to calibrate these signals into standard units, enabling comparison between FCMs. Figure 2 shows how

TABLE 1 | Overview of the performance of flow cytometers participating in the interlaboratory comparison study.

Flow cytometer	Data submitted	Passed scatter criterion	Passed fluorescence calibration		LoD			Flow rate				Group 1		Group 2	
			APC	PE	Optical EV diameter (nm)	APC (MESF)	PE (MESF)	MAD all beads (%)	MAD QC beads (%)	Based on	Passed flow rate criterion	APC	PE	APC	PE
Apogee A50-Micro	✓	✓			191			33	13	QC	✓				
Apogee A60-Micro	✓	✓		✓	121		1	18	13	QC	✓		✓		✓
Apogee A60-Micro	✓	✓	✓	✓	164	74	65	8	17	SNP	✓			✓	✓
Apogee A60-Micro-Plus	✓	✓	✓	✓	180	107	48	5	5	QC	✓			✓	✓
Apogee A60-Micro-Plus	✓	✓	✓	✓	180	83	43	2	2	QC	✓			✓	✓
Apogee A60-Micro-Plus	✓	✓	✓	✓	156	303	77	8	4	QC	✓			✓	✓
BC Astrios	✓	✓	✓	✓	139	773	35	5	3	QC	✓				✓
BC Cytoflex LX	✓	✓	✓	✓	152	194	11	21	11	QC	✓			✓	✓
BC Cytoflex LX	✓	✓	✓	✓	133	152	6	3	3	SNP	✓		✓	✓	✓
BC Cytoflex S	✓	✓	✓	✓	160	218	6	3	9	SNP	✓			✓	✓
BC Cytoflex S	✓	✓	✓	✓	344	297	74	33	25						
BC Cytoflex S	✓	✓	✓	✓	125	396	69	9	5	QC	✓			✓	✓
BC Cytoflex S	✓	✓	✓	✓	242	175	2	18	1	SNP	✓			✓	✓
BC Cytoflex S	✓	✓	✓	✓	113	24	11	2	1	SNP	✓	✓	✓	✓	✓
BC Cytoflex VBRY	✓	✓	✓	✓	234	183	8	32	30						
BD FACSCanto	✓														
BD FACSLyric	✓	✓	✓	✓	223	161	131	1	1	QC	✓			✓	

(Continues)

TABLE 1 | (Continued)

Flow cytometer	Data submitted	Passed scatter criterion	Passed fluorescence calibration		LoD			Flow rate				Group 1		Group 2	
			APC	PE	Optical EV diameter (nm)	APC (MESF)	PE (MESF)	MAD all beads (%)	MAD QC beads (%)	Based on	Passed flow rate criterion	APC	PE	APC	PE
BD FACSymphony A1 + SPD	✓	✓	✓	✓	94	96	16	5	2	SNP	✓	✓	✓	✓	✓
BD FACSymphony A1+ SPD	✓	✓	✓	✓	86	98	10	16	0	QC	✓	✓	✓	✓	✓
BD FACSymphony A1 + SPD	✓	✓	✓	✓	94	80	6	32	63						
BD FACSymphony A5	✓	✓	✓	✓	203	91	19	8	4	SNP	✓			✓	✓
Cytek Aurora + ESP	✓	✓	✓	✓	94	20	2	3	4	SNP	✓	✓	✓	✓	✓
Cytek Aurora+ ESP	✓	✓	✓	✓	90	39	3	12	7	QC	✓	✓	✓	✓	✓
Cytek Aurora	✓	✓	✓	✓	258	392	19	6	7	SNP	✓				
Cytek Aurora +ESP	✓	✓	✓	✓	104	20	1	14	1	QC	✓	✓	✓	✓	✓
Cytek Northern Lights +ESP	✓	✓	✓	✓	90	29	33	15	12	QC	✓	✓		✓	✓
12 instruments															

It is important to highlight that the reported LoDs reflect the assay's LoD. Laboratories were instructed to trigger on their most sensitive scatter detector but set the flow rate, detector voltage, laser powers, time interval after maintenance, and trigger threshold according to their own judgement. The performance of an FCM in this study does therefore not reflect the generic performance of a brand or type of FCM.Passed scatter criterion refers to an FCM capable of differentiating 125 nm polystyrene beads from 100 nm polystyrene beads or background noise by light scattering. Passed fluorescence calibration refers to an $R^2 > 0.98$. Passed flow rate criterion refers to an MAD for the flow rate based on either both SNPs and QC beads or QC beads alone >20 %. The "✓ " indicates that the specified criterion has been met. The "✓ " for group 1 or 2 for APC and PE refers to flow cytometers within the group boundaries that have ≥20 fluorescent-positive counts.

Abbreviations: APC, allophycocyanin; BC, Beckman Coulter; BD, Becton Dickinson Biosciences; ESP, enhanced small particle detection option; MAD, median absolute deviation; MESF, molecules of equivalent soluble fluorochrome; nm, nanometre; PE, phycoerythrin; QC, quality control; SNP, solid silica nanoparticles; SPD, Small Particle Detector.

fluorescence and light scattering calibrations were performed and how the LoDs of these detectors were determined.

Figure 2A shows the specified fluorescence intensity in molecules of soluble fluorophores (MESF) of reference particles versus the measured fluorescence intensity in arbitrary units for two detectors of an FCM. To calibrate the fluorescence detectors, that is, to relate the measured fluorescence intensities in arbitrary units to standard units of MESF, the log-transformed data were fitted with a linear function.

Figure 2B shows the measured light scattering intensity versus the diameter of polystyrene beads. The data were fitted with Mie theory, taking into account the diameter and refractive index of the beads as well as the optical configuration of the FCM (van der Pol et al. 2012). Based on this calibration, the scatter-to-diameter relationship of EVs was calculated, considering the low refractive index of EVs compared to beads (van der Pol et al. 2018). The dashed line was used to relate the measured scattering intensities of EVs to their optical diameter, which is the diameter of a spherical particle with a given refractive index that results in the measured light scattering signal.

To determine the LoD for both fluorescence and the optical diameter, which sets the threshold above which EVs can be detected, two empirical procedures are applied. Figure 2C shows how the LoD of the fluorescence detectors is determined. The figure shows the histogram of the calibrated fluorescence intensities for a PE detector. As the FCMs were triggered on light scattering, the bulk of the fluorescence intensity histogram represents the background noise. To quantify the LoD, the right flank of the background noise was fitted with a linear function and the *y*-intersect of the fit was multiplied by 3. The algorithm is validated, published and publicly available (Gankema et al. 2022).

To determine the LoD of the light scattering detector, the histogram of optical diameters of PEVTES was plotted, as shown in Figure 2D. As the number of particles increases with decreasing diameter below the LoD (van der Pol et al. 2014), the LoD was defined as the mode of the histogram. The procedures described in Figure 2 were applied to all FCMs in this study.

4.4 | Flow Cytometers Differ in Sensitivity

To compare EV concentrations in PEVTES within the same signal ranges, Table 1 and Figure 4A,B show the LoD for the APC and PE detectors in MESF, respectively, versus the LoD of the optical diameter in nm for all FCMs passing the inclusion criteria. The

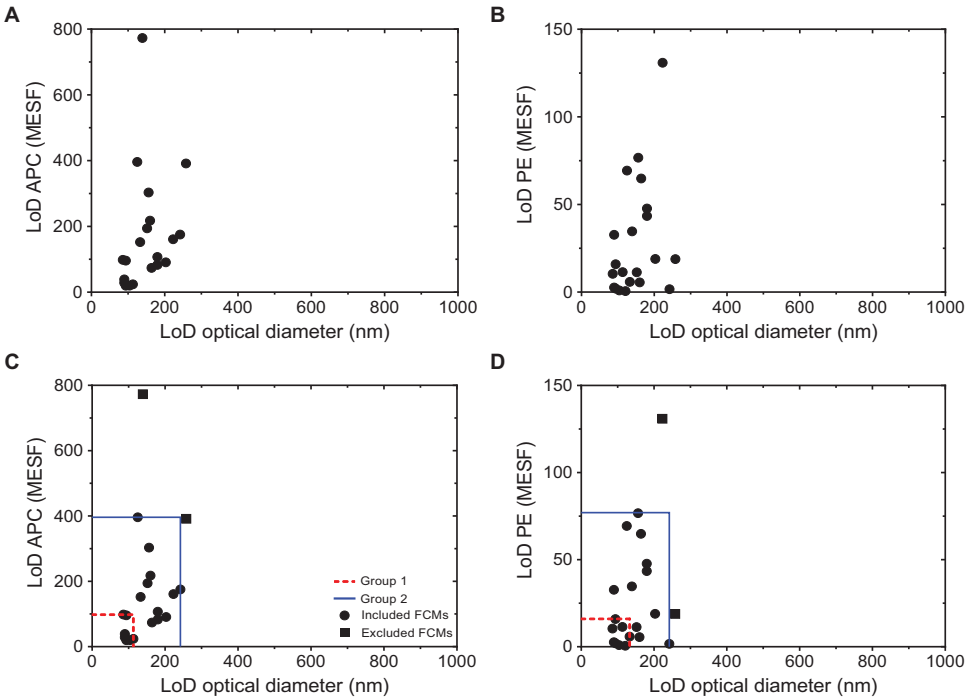

FIGURE 4 | Lower limit of detection (LoD) of calibrated fluorescence and light scattering detectors of flow cytometers [FCMs, ($n = 21$)] participating in the interlaboratory comparison study. (A) LoDs of the allophycocyanin (APC) and (B) phycoerythrin (PE) detectors versus the LoDs of the optical diameters for all participating FCMs (black circles). Calibrations and LoD determinations are explained in Figure 2. FCMs have different LoDs ranging between 20–773 MESF APC, 1–131 MESF PE and 86–258 nm EVs. (C-D) To compare cell-type-specific EV concentrations, FCMs were grouped by sensitivity. Group 1 includes the top-50 % most sensitive FCMs for each detector. Group 2 includes all FCMs that fall within 95th percentile of the LoD for calibrated fluorescence detectors and optical diameters. FCMs that did not fall within 95th percentile of the LoD of calibrated fluorescence detectors and optical diameters were considered unrepresentatively insensitive and were therefore excluded from further analysis. Excluded FCMs are depicted as black rectangles. Group 1 contains eight FCMs for PE and seven FCMs for APC, while group 2 contains 19 FCMs for PE and 18 FCMs for APC. To compare EV concentrations within similar fluorescence intensity and optical diameter ranges for both groups, gates equal to the least sensitive FCMs within each group were applied to the plasma EV test sample (PEVTES) data (Supporting Information 6). The gate applied to FCMs in group 1 is depicted by a red dashed line, and the gate for group 2 is shown as a blue solid line. Table 1 contains an overview of the included and excluded FCMs.

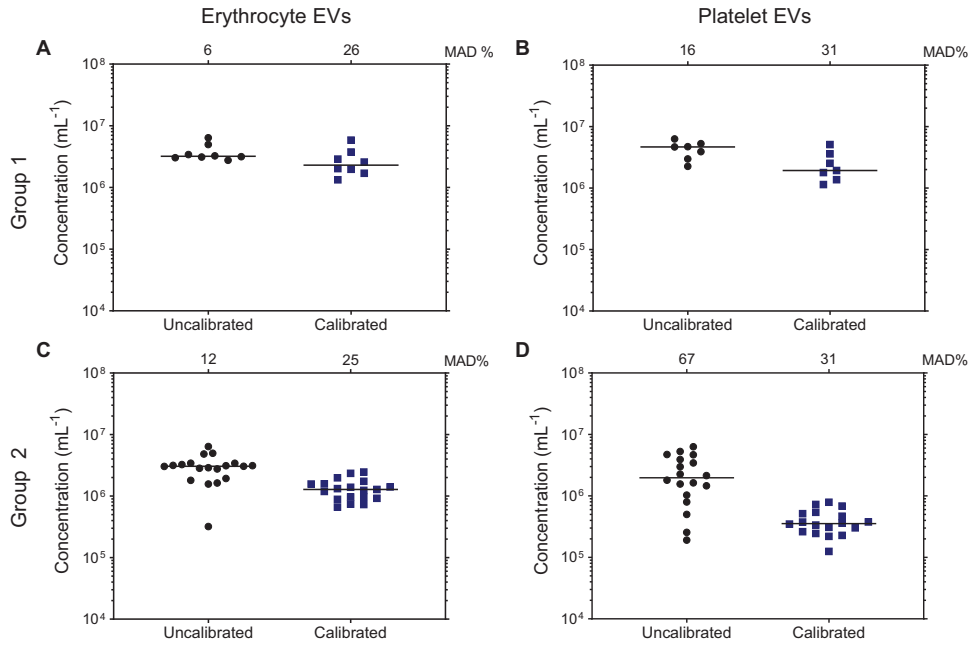

FIGURE 5 | Influence of calibration on the concentration of extracellular vesicles (EVs) in a 30-fold diluted plasma EV test sample (PEVTES) measured (symbols) with different flow cytometers (FCMs). The panels represent erythrocyte-derived [cluster of differentiation (CD) 235a-phycoerythrin (PE)] EVs in (A) group 1 (eight FCMs) and (C) group 2 (19 FCMs) and platelet-derived [CD61-allophycocyanin (APC)] in (B) group 1 (seven FCMs) and (D) group 2 (18 FCMs). Establishments of the groups is explained in Figure 4 and the Methods. The different symbols represent measured EV concentrations without calibration or application of gates (black circles), or with all aspects, that is, the flow rate, fluorescence detectors and light scattering detector calibrated (blue squares). Black lines indicate the median concentration. For the calibrated EV concentrations, different gates were applied. Calibrated EV concentrations in group 1 are reported with a fluorescence intensity >16 MESF PE and an optical diameter >133 nm for erythrocyte-derived EVs (A), a fluorescence intensity >98 MESF APC, and an optical diameter >113 nm for platelet-derived EVs (B). Calibrated EV concentrations in group 2 are reported with a fluorescence intensity of >77 MESF PE for erythrocyte-derived EVs and >396 MESF APCfor platelet-derived EVs, and an optical diameter >242 nm for both EV types. The variation of the measured concentrations was quantified using the median absolute deviation (MAD).

LoD range among FCMs is 39-fold for the APC detectors and 131-fold for the PE detectors, and 4-fold for the optical diameter, emphasizing that FCMs differ in sensitivity.

To compare FCMs with similar detector sensitivities, we divided all FCMs into two groups. Group 1 (red dashed lines) includes the top-50 % most sensitive FCMs regarding fluorescence and optical diameters. Group 2 (blue lines) includes all but the 5 % least sensitive FCMs, which are excluded to prevent insufficient EV counts (<20) at the remaining, more sensitive, FCMs. To compare EV concentrations within the same fluorescence intensity and size ranges, gates equal to the least sensitive FCMs in each group (red dashed lines and blue lines) were applied to the PEVTES data (Supporting Information 6).

4.5 | Comparable EV Concentrations by Calibration

After calibrating and grouping FCMs (Figures 2 and 4) and applying gates to select EVs with similar fluorescence intensities and optical diameters, we evaluated the impact of calibration on the variation of measured EV concentrations. Figure 5 shows the measured concentration of erythrocyte-, and platelet-derived EVs of FCMs in group 1 and 2 without calibration (black circles) and with calibration (blue squares). Considering the uncalibrated data in Figure 5, we conclude that just selecting and grouping FCMs by sensitivity decreases the variation of the measured EV concentrations compared to the inclusion of all FCMs (Figure 3). For erythrocyte-derived EVs, the MAD reduced from 30 % (Figure 3) to 6 % for group 1 (Figure 5A) and to 12 % for group 2 (Figure 5C). For platelet-derived EVs, grouping reduced the MAD from 72 % (Figure 3) to 16 % for group 1 (Figure 5B) and to 67 % for group 2 (Figure 5D).

Six out of eight FCMs in group 1 measured nearly the same concentration of erythrocyte-derived EVs (Figure 5A), even without calibration, suggesting that these FCMs have the sensitivity to detect most if not all erythrocyte-derived EVs. The resulting MAD is so low that calibration statistically increased the variation. However, the range of the measured erythrocyte-derived EV concentration of group 2 visibly decreases, which is confirmed by a decreasing COR (Supporting Information 7). Hence, calibration seems to correct for outliers. Moreover, calibration reduced the MAD of uncalibrated and ungrouped data from 30 % (Figure 3) to 26 % for group 1 (Figure 5A) and to 25 % for group 2 (Figure 5C).

For platelet-derived EVs in both group 1 (Figure 5B) and group 2 (Figure 5D), calibration leads to an MAD of 31 %, which is substantially lower than the MAD of 72 % for uncalibrated and ungrouped data (Figure 3). For platelet-derived EVs in group 2, calibration decreased the variation of the measured EV concentrations compared to uncalibrated and ungrouped, as expected.

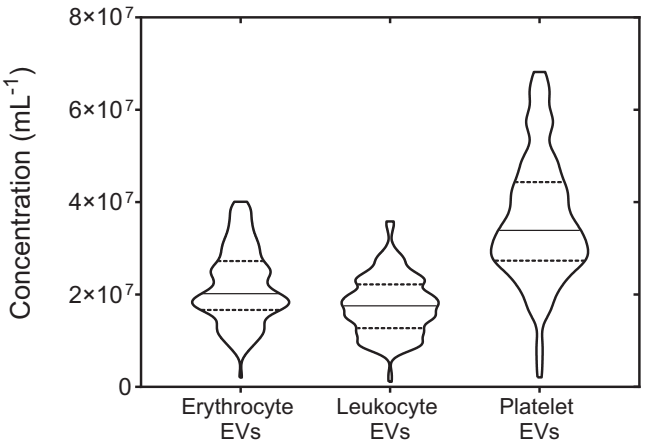

FIGURE 6 | Reference ranges of the concentration of erythrocyte-derived, leukocyte-derived and platelet-derived extracellular vesicles (EVs) in blood plasma of 224 healthy human individuals. Erythrocyte-derived EVs were stained with cluster of differentiation (CD) 235a-phycoerythrin (PE), leukocyte-derived EVs with CD45-allophycocyanin (APC), and platelet-derived EVs with CD61-brilliant violet (BV) 421 and measured on an Apogee A60-Micro flow cytometer (Apogee Flow Systems). The violin plots show the median (centre line), the first quartile (dashed lower line, Q1, 25th percentile) and the third quartile (dashed upper line, Q1, 75th percentile) of the measured concentration of EVs. EV concentrations are reported with a fluorescence intensity >112 MESF APC, >77 MESF BV421, and >228 MESF PE, and an optical diameter between 150 and 1000 nm per/mL of cell-depleted human blood plasma. Calibrations and establishment of the LoDs were performed as explained in Figure 2.

In sum, especially for small and dim particles like EVs calibration is needed to determine the LoDs of FCM detectors and thereby group FCMs by sensitivity, which in turn reduces the variation of measured EV concentrations in the same sample. Applying the full calibration methodology validated in this study reduces the MAD and the range, expressed as COR of all investigated groups compared to uncalibrated and ungrouped data.

4.6 | Reference Ranges of EV Concentrations

The calibration methodology enables conversion of arbitrary units of fluorescence and light scattering into comparable units, thereby providing a solid foundation to compare EV concentrations between different FCMs and laboratories. To demonstrate the clinical applicability of the methodology, we established reference ranges of blood cell-derived EV concentrations in blood plasma of 224 healthy human individuals. All samples were measured on one FCM (Apogee A60-Micro, Apogee Flow Systems) to which the calibration methodology was applied. Figure 6 shows the reference ranges of the concentration of erythrocyte-derived (CD235a-PE), leukocyte-derived (CD45-APC), and platelet-derived (CD61-BV421) EVs within well-defined signal ranges.

The reference ranges for (1) erythrocyte-derived EVs is 8.54 •10^6 – 3.88 • 10^7 EVs/mL, with a median concentration of 2.02 • 10^7 EVs/mL, (2) leukocyte-derived EVs is 7.58 • 10^6 – 3.03 • 10^7 EVs/mL with a median concentration of 1.75 •10^7 EVs/mL, and (3) platelet-derived EVs is 1.01 • 10^7 – 6.57 • 10^7 EVs/mL with a median concentration of 3.39 • 10^7 EVs/mL in cell-depleted human blood plasma. These concentration ranges apply to EVs with a fluorescence intensity >228 MESF PE for erythrocyte-derived EVs, >112 MESF APC for leukocyte-derived EVs, and >77 MESF BV421 for platelet-derived EVs, and an optical diameter between 150 and 1000 nm.

5 | Discussion

5.1 | Challenges in Comparing EV Concentrations Across Flow Cytometers

EV concentrations in human blood plasma have been explored as potential disease biomarkers for over 25 years. Despite numerous interlaboratory comparison studies, EV concentrations remain incomparable across FCMs and laboratories. To measure reliable and comparable EV concentrations, we validated a methodology that involves calibration of the flow rate and FCM detectors. The methodology was evaluated in a global interlaboratory comparison study, including 25 FCMs from 18 laboratories. We then applied the methodology to establish reference ranges for blood cell-derived EV concentrations in human blood plasma from 224 healthy individuals, demonstrating its clinical feasibility.

Comparing EV concentrations between FCMs is challenging, because FCM data have arbitrary units. Without calibration, EV concentrations measured in the same sample with 25 different FCMs span roughly two orders of magnitude, with the MAD ranging from 30 % for erythrocyte-derived EVs to 72 % for platelet-derived EVs (Figure 3). The variation in uncalibrated data is lower than expected for a dataset in arbitrary units, which is by definition not comparable. For example, reported concentrations of platelet-derived EVs measured with different uncalibrated FCMs differ three orders of magnitude (Yuana et al. 2010; Gasecka et al. 2017). The unexpectedly low variation in our study may be attributed to the inclusion criterion requiring participants to have an FCM capable of differentiating 125 nm polystyrene beads from 100 nm polystyrene beads or background noise by light scattering. This criterion effectively pre-selected FCMs with a comparable sensitivity, thereby improving data comparability. Additionally, automated software was used to standardize the gating of the arbitrary unit data, which likely further reduced variation. Furthermore, the use of ready-to-measure PEVTES likely further reduced variation by minimizing operator-introduced and sample preparation variation (see Section on 'Comparison With Previous Interlaboratory Comparison Studies').

5.2 | Impact of Calibration on Measurement Reproducibility

We applied the calibration methodology (Figure 2) to determine the LoD of the fluorescence and light scattering detectors of each FCM. Figure 4 and Table 1 show that the sensitivity of detectors differs between FCMs. The sensitivity of an FCM is influenced by its hardware, maintenance state, and applied settings, all of which depend on the operator's experience. We assumed that all laboratories optimized their FCMs for small particle detection. Thus, the reported LoDs reflect the assay's LoD rather than the instrument's physical LoD. Consequently, the FCM performance

reported in this study does not reflect the generic performance of a brand or FCM model. Importantly, by applying calibration, differences in flow rate, detector voltage, laser power, and other acquisition settings are accounted for, allowing for quantitative comparisons independent of instrument-specific configurations.

After assessing the sensitivity of all FCMs, FCMs were divided into two sensitivity-based groups (Figure 4C,D). We then evaluated the impact of the calibration methodology on the variation of the measured EV concentrations (Figure 5). Grouping FCMs with similar sensitivities decreased the variation, even without applying gates in standard units, compared to including all FCMs (Figures 3 and 5). This finding emphasizes the need for calibration, as grouping FCMs with similar sensitivities can only be done in standard units.

The variation in uncalibrated erythrocyte-derived EV concentration was unexpectedly low (Figure 5). One possible explanation is that FCMs (group 1) are sufficiently sensitive to detect most, if not all, erythrocyte-derived EVs. In group 1, the optical diameter gate was set at ≥133 nm, which is slightly below the reported peak of the size distribution for erythrocyte-derived EVs (150–200 nm) (Varga et al. 2014). As a result, most, if not all, erythrocyte-derived EVs are detected.

Applying the calibration methodology resulted in MADs of 25 % for erythrocyte-derived EVs and 31 % for platelet-derived EVs (Figure 5C,D). Thus, the methodology allows to measure comparable EV concentrations across different FCMs and laboratories, compared to previously reported EV concentrations spanning orders of magnitudes (Yuana et al. 2010; Gasecka et al. 2017).

5.3 | Comparison With Previous Interlaboratory Comparison Studies

Over the past decade, several interlaboratory studies were performed with the goal to standardize EV concentration measurements with flow cytometry (van der Pol et al. 2018; Robert et al. 2009; Bettin et al. 2023; Lacroix et al. 2010; Cointe et al. 2017; Welsh, Jones, et al. 2020). In these studies, however, either none, one (flow rate), or two (flow rate and light scattering) of the three parameters of an EV flow cytometry measurement were calibrated. In an interlaboratory comparison study performed in 2018 using pre-defined EV diameter ranges, both flow rate and light scattering calibration were performed, but no fluorescence calibration (van der Pol et al. 2018). For the first time, in 2020, Welsh et al. calibrated the flow rate, fluorescence and light scattering signal of FCMs (Welsh, Jones, et al. 2020). Although the study showed that simultaneous calibration of the flow rate, fluorescence and light scattering signal reduces variability, this study included only two instruments.

Furthermore, none of the previous interlaboratory comparison studies included a ready-to-measure EV test sample. Instead, frozen aliquots of, for example, plasma were distributed and participants had to stain EVs themselves, thereby introducing additional pre-analytical and inter-operator variability (van der Pol et al. 2018; Bettin et al. 2023). A ready-to-measure and stable sample such as PEVTES that was used in our present study, eliminates this additional source of variation.

Additionally, from our present study, it is clear that the sensitivity of FCMs increased substantially over the past years (Figure 4). In 2018, another interlaboratory comparison study aimed to standardize EV concentration measurements in human blood plasma by diameter approximation. In this study from van der Pol et al., 6 out of 46 FCMs could detect EVs with a diameter of 300 nm (van der Pol et al. 2018). In our study, 24 out of 25 FCMs could at least detect 300 nm EVs. Additionally, 6 out of 25 FCMs were able to detect EVs as small as 100 nm and 19 FCMs could detect EVs of 200 nm. This outcome indicates that modern FCMs are more sensitive and/or that researchers have improved knowledge and better tools at hand, such as RMs, to select more suitable FCMs to characterize EVs.

Over the last decade(s), the EV flow cytometry field has progressed from irreproducible single-centre studies without calibration, to partial signal calibration, and to a small number of studies applying full instrument calibration. Although uncalibrated data are still frequently published, our study demonstrates that full instrument calibration enables reproducible concentration measurements across different instruments.

5.4 | Establishing Reference Ranges for EV Concentrations in Healthy Individuals

To validate the potential of EV concentration-based biomarkers, we established reference ranges of blood cell-derived EV concentrations in blood plasma from 224 healthy individuals (Figure 6). The EV concentrations reported in this manuscript are valid only within the specified fluorescence intensities and optical diameter ranges and are, therefore, reproducible. The established reference ranges need to be validated using different FCMs and in other laboratories. Laboratories with more sensitive FCMs than ours should then apply gates to select EVs within the same signal range as our FCM. To allow laboratories with less sensitive FCMs than our FCM to compare EV concentrations to the established reference values, we are currently developing a three-dimensional matrix, relating EV concentration reference ranges to both the fluorescence intensity LoD and the optical diameter LoD. This three-dimensional matrix will enable users to look up the reference ranges of cell-derived EV concentrations in blood plasma that a given FCM is expected to measure, based on the LoDs of the FCM.

EV concentrations can be affected by various factors. Biospecimen factors including clinical, demographic, and lifestyle factors, may impact measured EV concentrations. Additionally, pre-analytical variables, such as blood sample collection, handling, and processing play a role (Lucien et al. 2023; Dhondt et al. 2023; Coumans et al. 2017). Analytical variables, including the choice of antibodies and fluorochromes, as well as the antibody concentration added to the sample also contribute to variability, as the fluorescence intensity of stained EVs depends on both the number and brightness of the selected fluorophore (Welsh et al. 2023; Pink et al. 2023). Further research is needed to determine how biospecimen factors, pre-analytical variables, and analytical variables impact blood EV concentrations. Quantifying these effects requires calibration-based studies to ensure comparability and reproducibility. Thus, the calibration methodology presented in this manuscript offers a tool to systematically investigate the

effects of both biospecimen factors and pre-analytical variables on EV concentrations.

A recently published study from Holcar et al. comprehensively characterized EVs in blood plasma from 208 healthy humans. They explored the cellular origin and biological variation of EVs in blood plasma, thereby providing valuable insights into the composition and characteristics of EVs in health (Holcar et al. 2025). However, compared to our study, the LoDs of the imaging FCM used, as well as the fluorescence and size ranges in which the measured EV concentrations were determined, were not reported, which makes it difficult to compare their results to ours and other (future) studies.

5.5 | Improving Reproducibility in EV Research Through Education

Reliable and reproducible EV concentration measurements with flow cytometry require implementation of best practices in small particle flow cytometry, including calibration. The calibration methodology presented in this study enables researchers to generate comparable and reproducible datasets across instruments and laboratories. Calibration can be applied to any FCM to: (1) convert arbitrary measurement units into standard units, and (2) quantitatively assess the instrument performance and limitations. Importantly, calibration can be applied to any FCM, not only to those included in the present study. For light scatter calibration, software supporting most instruments (though not yet imaging FCMs) is available, such as Rosetta Calibration (Exometry, Netherlands) and FCM_{PASS} (Welsh, Tang, et al. 2020; Welsh, Tang, et al. 2020). In the present study, calibration also allowed us to assign instruments to sensitivity-based groups for comparison. Such groups are study-specific and should be adapted per study.

A key prerequisite for implementation of calibration requires knowledge dissemination on best practices. Scientific societies such as the International Society for Extracellular Vesicles (ISEV) and the International Society for the Advancement of Cytometry (ISAC), along with inter-society working groups like the EV Flow Cytometry Working Group or ISEV's Scientific Reproducibility Task Forces, actively promote reproducibility. They do so by organizing conferences, and workshops, and by publishing guidelines and position papers. ISEV also supports education through initiatives like the annual Education Day, while specialized summer schools, such as those organized by for instance, the Amsterdam Vesicle Centre or UCD Conway Institute, offer hands-on training in EV flow cytometry. In addition, guidelines, position papers, and frameworks promote transparent reporting to further facilitate reproducibility. Examples include the MIFlowCyt-EV (Welsh et al. 2021; Welsh, van der Pol, et al. 2020) for standardized reporting of EV flow cytometry experiments, the Compendium of single EV flow cytometry (Welsh et al. 2023) for best practices in small particle detection, or the MIBlood-EV (Lucien et al. 2023) for reporting of blood EV studies. Overall, education and knowledge transfer from experts are essential to enhance the quality and reproducibility of EV research.

5.6 | Applicability of the Calibration Methodology Beyond EV Research

The calibration methodology presented in this manuscript offers a standardization approach that is also applicable beyond blood plasma and EV research. All small particles and fluids that are flow cytometry compatible, such as bacteria, viruses, and small cells in urine, saliva, and other fluids, can benefit from the methodology though modifications may be necessary to accommodate differences in particle properties. An example is a Dutch multicentre study aiming to standardize and quantify platelet activation with flow cytometry in patients with inherited platelet function defects. Generally, any study investigating factors that may influence EV concentrations, such as but not limited to pre-analytical or analytical variables, will benefit from the developed calibration methodology.

5.7 | Limitations and Future Perspectives

The methodology validated in this manuscript allows for measuring comparable and reproducible EV concentrations with flow cytometry. Although it is not necessary for users to use the exact QC materials and calibration beads used in this study, users should select appropriate materials that align with their specific needs and experimental setup. RMs should have a specified quantity value, ideally accompanied with a known uncertainty (Welsh et al. 2023; Bettin et al. 2023). However, commercially available submicrometer RMs with traceable particle concentrations for flow rate calibrations, or traceable size and refractive index for light scattering calibrations, are currently unavailable. Similarly, small and dim beads for fluorescence calibration are lacking. Dedicated EV RMs mimicking EVs' physical properties, with known uncertainties, are essential for reliable calibration of vesicle flow cytometry (Bettin et al. 2023; JCGM 2008; Deumer et al. 2024). Calibration beads that come with assigned uncertainties differ in their uncertainty values, and these differences in uncertainty can affect the calibration and influence the reported EV concentrations (Welsh et al. 2023; van der Pol et al. 2018; Bettin et al. 2023). How much these differences influence calibration procedures and reported EV concentrations; however, remains to be investigated. Establishing full uncertainty budgets including the uncertainties of (1) calibration beads, (2) calibration procedures, and (3) instrument performance, enable identification of (dominant) error sources and improve the accuracy and comparability of EV concentration measurements.

A limitation of this study was the flow rate determination and its stability during the PEVTES measurement. Traceable spike-in counting beads could help address this shortcoming in the future. Additionally, RMs mimicking EVs' physical properties and traceable RI determination for both RMs and EVs would further enhance data reliability and comparability (Deumer et al. 2024). Ideally, a single tube would contain three types of beads with known uncertainties to calibrate the flow rate, fluorescence, and light scattering, into which the EV-containing sample could be added. However, such tubes are currently unavailable.

In the present study, the focus was on inter-FCM variability, while intra-FCM variability will be addressed in future work.

Generally, calibration resulted in MADs of 25 % for erythrocyte-derived EVs and 31 % for platelet-derived EVs on 25 different FCMs. This result exceeded our expectations, because reported concentrations of platelet-derived EVs differed 1000-fold between 1997 and 2014 (Vis and Huisman 2016) and size calibration alone lead to a CV of 81 % for EV concentrations (van der Pol et al. 2018). Although we are not yet at the level of laboratory tests, which typically have uncertainties of ≤10 %–15 % (2025 CLIA Acceptance Limits for Proficiency Testing—Westgard QC; International Organization for Standardization 2013; Vis and Huisman 2016), a direct comparison cannot be made, because our reported MADs describe the reproducibility of a measurement, whereas reported uncertainties of laboratory tests include both the reproducibility and measurement bias. Nevertheless, our results demonstrate that reproducible EV concentration measurements are feasible across instruments. The achieved MADs are an important first step toward EV-based biomarker research, and they may be tolerated in exploratory research rather than for clinical decision-making. Their acceptability ultimately depends on the specific research questions and whether biological differences between patient groups or healthy individuals exceed this level of variability. Bringing EV quantification closer to the acceptable variability levels required for research and clinical applications demonstrates the progress achieved in this study, while also highlighting the ongoing challenge of obtaining reproducible concentrations for a heterogenous analyte such as EVs. Whether clinically acceptable variability can ultimately be achieved, remains to be investigated.

In summary, we validated a methodology to measure reliable and comparable EV concentrations by flow cytometry in the biggest global interlaboratory EV comparison study to date. The methodology not only enables reproducible cell-type-specific EV concentration measurements, but also opens the door for exploring EV concentration-based diagnostic and therapeutic applications in the future. To demonstrate the clinical applicability of the methodology, we determined reference ranges of blood cell-derived EV concentrations, within well-defined fluorescence and size ranges, in blood plasma from 224 healthy humans.

Recommendations (to Achieve Reproducible EV Concentrations With Flow Cytometry)

- Calibrate the flow cytometer's flow rate, fluorescence signals, and light scattering signals using reference materials.
- Implement quality controls to monitor instrument performance and ensure measurement reliability.
- Use assay controls to verify that the detected signals originate from EVs.
- Report EV concentrations in well-defined fluorescence and size ranges to allow comparison across FCMs and laboratories.
- Transparently report all details specific to your study, including pre-analytical variables and experimental design, sample preparation, used (assay) controls, details on calibration, data acquisition, and analysis. For help on what to report, use checklists like the MIFlowCyt-EV framework (Welsh et al. 2021; Welsh, van der Pol, et al. 2020) and MIBlood-EV (Lucien et al. 2023).

Author Contributions

Britta A. Bettin: conceptualization, data curation, formal analysis, investigation, project administration, visualization, writing – original draft, writing – review and editing. **Bo Li**: writing – review and editing. **Kim Falkena**: data curation, formal analysis, writing – review and editing. **Ton G. van Leeuwen**: conceptualization, writing – review and editing. **Christian Gollwitzer**: writing – review and editing. **Zoltán Varga**: writing – review and editing. **Nadine Ajzenberg**: investigation, writing – review and editing. **Pascale Berckmans**: investigation, writing – review and editing. **Randy P. Carney**: investigation, writing – review and editing. **Sean Cook**: investigation. **Françoise Dignat-george**: investigation, writing – review and editing. **Dorothee Faille**: investigation, writing – review and editing. **Bernd Giebel**: investigation, writing – review and editing. **Jennifer C. Jones**: investigation, writing – review and editing. **Yohan Kim**: investigation, writing – review and editing. **Romaric Lacroix**: investigation, writing – review and editing. **Joanne Lannigan**: investigation, writing – review and editing. **Fabrice Lucien**: investigation, writing – review and editing. **Katariina Maaninka**: investigation, writing – review and editing. **Erika G. Marques de Menezes**: investigation, writing – review and editing. **Annette Meyer**: investigation, writing – review and editing. **Rachel R. Mizenko**: investigation, writing – review and editing. **Inge Nelissen**: investigation, writing – review and editing. **John Nolan**: investigation, writing – review and editing. **Philip J. Norris**: investigation, writing – review and editing. **Desmond Pink**: investigation, writing – review and editing. **Sumeet Poudel**: investigation, writing – review and editing. **Stéphane Robert**: investigation, writing – review and editing. **Vera A. Tang**: investigation, writing – review and editing. **Tobias Tertel**: investigation, writing – review and editing. **Tina Van Den Broeck**: investigation, writing – review and editing. **Lili Wang**: investigation, writing – review and editing. **Rienk Nieuwland**: conceptualization, funding acquisition, project administration, visualization, writing – original draft, writing – review and editing. **Edwin van der Pol**: conceptualization, data curation, formal analysis, funding acquisition, project administration, visualization, writing – original draft, writing – review and editing.

Acknowledgements

We would like to thank the 18HLT01: METVES II consortium for their invaluable support. We especially thank, Anikó Gaál from the Institute of Materials and Environmental Chemistry, Research Centre for Natural Sciences, Budapest, Hungary, for developing the solid silica nanoparticles. Furthermore, we would like to thank Robin Schürmann from Physikalisch-Technische Bundesanstalt, Berlin, Germany and Dorota Bartczak from National Measurement Laboratory, LGC Limited, Teddington, United Kingdom, for the traceable characterization of the solid silica nanoparticles. We thank John P Nolan from Cellarcus Biosciences for the contribution of vCal Nanorainbow Beads and BD Biosciences for the contribution of MESF beads which were provided under the 18HLT01 METVES II European Union's Horizon 2020 Research and Innovation Program contract where BD Biosciences was an unfunded partner. Rienk Nieuwland and Edwin van der Pol share senior authorship.

Funding

Britta A. Bettin acknowledges funding for project 18HLT01: METVES II, which has received funding from the EMPIR program co-financed by the participating states and from the European Union's Horizon 2020 Research and Innovation Program. Edwin van der Pol acknowledges funding from the Dutch Research Council (NWO) for VIDI project 19724.

Conflicts of Interest

Edwin van der Pol is a cofounder and shareholder of the company Exometry B.V. (Amsterdam, The Netherlands). Joshua A. Welsh is an employee of BD Biosciences and Director of The Measuring Stick, Ltd. John P. Nolan is a Professor at the Scintillon Institute and CEO of Cellarcus Biosciences. Tina Van Den Broeck is employee of BD Biosciences, the manufacturer of the MESF beads used, and was operator for one of the 3 FACSymphony A1 measurements in the interlaboratory study. Joanne Lannigan has been a consultant for Cytek Biosciences and is currently on their Scientific Advisory Board.

Data Availability Statement

The data that support the findings will be available in Figshare at https://figshare.com/s/9a847bd8ede732ba9c1e following an embargo from the date of publication to allow for commercialization of research findings.

References

Exosome Technologies Market Size, Share & Forecast - 2031. https://www.transparencymarketresearch.com/exosome-technologies-market.html.

2025 CLIA Acceptance Limits for Proficiency Testing—Westgard QC. https://westgard.com/clia-a-quality/quality-requirements/2024-clia-requirements.html?utm_source=chatgpt.com.

Abbott, A. 2023. "FedEx for Your Cells: This Biological Delivery Service Could Treat Disease." *Nature* 621: 462–464.

Arraud, N., R. Linares, S. Tan, et al. 2014. "Extracellular Vesicles From Blood Plasma: Determination of Their Morphology, Size, Phenotype and Concentration." *Journal of Thrombosis and Haemostasis* 12: 614–627.

Berezin, A. E., A. A. Kremzer, T. A. Samura, et al. 2015. "Predictive Value of Apoptotic Microparticles to Mononuclear Progenitor Cells Ratio in Advanced Chronic Heart Failure Patients." *Journal of Cardiology* 65: 403–411.

Bettin, B., E. van der Pol, and R. Nieuwland. 2023. "Plasma Extracellular Vesicle Test Sample to Standardize Flow Cytometry Measurements." *Research and Practice in Thrombosis and Haemostasis* 7: 100181.

Bettin, B. A., Z. Varga, R. Nieuwland, and E. van der Pol. 2023. "Standardization of Extracellular Vesicle Concentration Measurements by Flow Cytometry: The Past, Present, and Future." *Journal of Thrombosis and Haemostasis* 21: 2032–2044. https://doi.org/10.1016/j.jtha.2023.04.042.

Bray, F., M. Laversanne, E. Weiderpass, and I. Soerjomataram. 2021. "The Ever-Increasing Importance of Cancer as a Leading Cause of Premature Death Worldwide." *Cancer* 127: 3029–3030.

Buntsma, N. C., A. Gąsecka, Y. B. W. E. M. Roos, T. G. van Leeuwen, E. van der Pol, and R. Nieuwland. 2022. "EDTA Stabilizes the Concentration of Platelet-Derived Extracellular Vesicles During Blood Collection and Handling." *Platelets* 33: 764–771.

Buntsma, N. C., M. Shahsavari, A. Gąsecka, R. Nieuwland, T. G. van Leeuwen, and E. Van Der Pol. 2023. "Preventing Swarm Detection in Extracellular Vesicle Flow Cytometry: A Clinically Applicable Procedure." *Research and Practice in Thrombosis and Haemostasis* 7: 100171.

Caby, M.-P., D. Lankar, C. Vincendeau-Scherrer, G. Raposo, and C. Bonnerot. 2005. "Exosomal-Like Vesicles Are Present in Human Blood Plasma." *International Immunology* 17: 879–887.

Chandler, W. L., W. Yeung, and J. F. Tait. 2011. "A New Microparticle Size Calibration Standard for Use in Measuring Smaller Microparticles Using a New Flow Cytometer." *Journal of Thrombosis and Haemostasis* 9: 1216–1224.

Chatterjee, M., S. Özdemir, C. Fritz, et al. 2024. "Plasma Extracellular Vesicle Tau and TDP-43 as Diagnostic Biomarkers in FTD and ALS." *Nature Medicine* 30: 1771–1783.

Cointe, S., C. Judicone, S. Robert, et al. 2017. "Standardization of Microparticle Enumeration Across Different Flow Cytometry Platforms: Results of a Multicenter Collaborative Workshop." *Journal of Thrombosis and Haemostasis* 15: 187–193.

Coumans, F. A. W., A. R. Brisson, E. I. Buzas, et al. 2017. "Methodological Guidelines to Study Extracellular Vesicles." *Circulation Research* 120: 1632–1648.

Daimon, M., and A. Masumura. 2007. "Measurement of the Refractive Index of Distilled Water From the Near-Infrared Region to the Ultraviolet Region." *Applied Optics* 46: 3811.

de Rond, L., F. A. W. Coumans, R. Nieuwland, T. G. van Leeuwen, and E. van der Pol. 2018. "Deriving Extracellular Vesicle Size From Scatter Intensities Measured by Flow Cytometry." *Current Protocols and Cytometry* 86: e43.

de Rond, L., E. van der Pol, C. M. Hau, et al. 2018. "Comparison of Generic Fluorescent Markers for Detection of Extracellular Vesicles by Flow Cytometry." *Clinical Chemistry* 64: 680–689.

Deumer, J., R. Schürmann, A. Gaál, et al. 2024. "Traceable Characterization of Hollow Organosilica Beads as Potential Reference Materials for Extracellular Vesicle Measurements With Optical Techniques." *Discover Nano* 19: 14.

Dhondt, B., C. Pinheiro, E. Geeurickx, et al. 2023. "Benchmarking Blood Collection Tubes and Processing Intervals for Extracellular Vesicle Performance Metrics." *Journal of Extracellular Vesicles* 12: e12315.

Doornbos, R. M. P., A. G. Hoekstra, K. E. I. Deurloo, B. G. de Grooth, P. M. A. Sloot, and J. Greve. 1994. "Lissajous-Like Patterns in Scatter Plots of Calibration Beads." *Cytometry* 16: 236–242.

Enciso-Martinez, A., C. Løppke, J. J. Koene, et al. 2025. "Targeting Oncofoetal Chondroitin Sulphate Allows Identification of Tumour-Derived Extracellular Vesicles." *Journal of Extracellular Vesicles* 14: e70106.

Exosomes Market Size & Share—Trends Analysis Report. 2032. https://www.gminsights.com/industry-analysis/exosomes-market.

Fais, S., L. O'Driscoll, F. E. Borras, et al. 2016. "Evidence-Based Clinical Use of Nanoscale Extracellular Vesicles in Nanomedicine." *ACS Nano* 10: 3886–3899.

Gankema, A. A. F., B. Li, R. Nieuwland, and E. Pol. 2022. "Automated Fluorescence Gating and Size Determination Reduce Variation in Measured Concentration of Extracellular Vesicles by Flow Cytometry." *Cytometry Part A* 101: 1049–1056.

Gasecka, A., A. N. Böing, K. J. Filipiak, and R. Nieuwland. 2017. "Platelet Extracellular Vesicles as Biomarkers for Arterial Thrombosis." *Platelets* 28: 228–234.

Holcar, M., I. Marić, T. Tertel, et al. 2025. "Comprehensive Phenotyping of Extracellular Vesicles in Plasma of Healthy Humans—Insights into Cellular Origin and Biological Variation." *Journal of Extracellular Vesicles* 14: e70039.

Horn, P. S., and A. J. Pesce. 2003. "Reference Intervals: An Update." *Clinica Chimica Acta* 334: 5–23.

Hoshino, A., H. S. Kim, L. Bojmar, et al. 2020. "Extracellular Vesicle and Particle Biomarkers Define Multiple Human Cancers." *Cell* 182: 1044–1061.e18.

International Organization for Standardization. 2013. *ISO 15197:2013(En), In Vitro Diagnostic Test Systems — Requirements for Blood-Glucose Monitoring Systems for Self-Testing in Managing Diabetes Mellitus*. https://www.iso.org/standard/54976.html.

JCGM. 2008. "JCGM 200: 2008 International Vocabulary of Metrology — Basic and General Concepts and Associated Terms (VIM) Vocabulaire International De Métrologie — Concepts Fondamentaux Et Généraux Et Termes Associés (VIM)." *International Organization for Standardization* 3: 104.

Kasarova, S. N., N. G. Sultanova, C. D. Ivanov, and I. D. Nikolov. 2007. "Analysis of the Dispersion of Optical Plastic Materials." *Optical Materials (Amst)* 29: 1481–1490.

Lacroix, R., S. Robert, P. Poncelet, R. S. Kasthuri, N. S. Key, and F. Dignat-George. 2010. "Standardization of Platelet-Derived Microparticle Enumeration by Flow Cytometry With Calibrated Beads: Results of the International Society on Thrombosis and Haemostasis SSC Collaborative Workshop." *Journal of Thrombosis and Haemostasis* 8: 2571–2574.

Li, J., C. A. Sherman-Baust, M. Tsai-Turton, R. E. Bristow, R. B. Roden, and P. J. Morin. 2009. "Claudin-Containing Exosomes in the Peripheral Circulation of Women With Ovarian Cancer." *BMC Cancer* 9: 244.

Logozzi, M., A. de Milito, L. Lugini, et al. 2009. "High Levels of Exosomes Expressing CD63 and Caveolin-1 in Plasma of Melanoma Patients." *PLOS ONE* 4: e5219.

Loyer, X., A.-C. Vion, A. Tedgui, and C. M. Boulanger. 2014. "Microvesicles as Cell–Cell Messengers in Cardiovascular Diseases." *Circulation Research* 114: 345–353.

Lucien, F., D. Gustafson, M. Lenassi, et al. 2023. "MIBlood-EV: Minimal Information to Enhance the Quality and Reproducibility of Blood Extracellular Vesicle Research." *Journal of Extracellular Vesicles* 12: 12385.

Nanou, A., F. A. W. Coumans, G. van Dalum, et al. 2018. "Circulating Tumor Cells, Tumor-Derived Extracellular Vesicles and Plasma Cytokeratins in Castration-Resistant Prostate Cancer Patients." *Oncotarget* 9: 19283–19293.

Pink, D., A. Basu, M. Wong, et al. 2023. "Antibody Titrations Are Critical for Microflow Cytometric Analysis of Extracellular Vesicles." *Cytometry Part A* 103: 670–683.

Raj, D. A. A., I. Fiume, G. Capasso, and G. Pocsfalvi. 2012. "A Multiplex Quantitative Proteomics Strategy for Protein Biomarker Studies in Urinary Exosomes." *Kidney International* 81: 1263–1272.

Robert, S., P. Poncelet, R. Lacroix, et al. 2009. "Standardization of Platelet-Derived Microparticle Counting Using Calibrated Beads and a Cytomics FC500 Routine Flow Cytometer: A First Step Towards Multicenter Studies?" *Journal of Thrombosis and Haemostasis* 7: 190–197.

Schürmann, R., A. Gaál, A. Sikora, et al. 2024. "Comparing Novel Small-Angle X-Ray Scattering Approaches for Absolute Size and Number Concentration Measurements of Spherical SiO2 Particles to Established Methods." *Nanotechnology* 35: 385701.

Sódar, B. W., Á. Kittel, K. Pálóczi, et al. 2016. "Low-Density Lipoprotein Mimics Blood Plasma-Derived Exosomes and Microvesicles During Isolation and Detection." *Scientific Reports* 6: 24316.

Tian, Y., M. Gong, Y. Hu, et al. 2020. "Quality and Efficiency Assessment of Six Extracellular Vesicle Isolation Methods by Nano-Flow Cytometry." *Journal of Extracellular Vesicles* 9: 1697028.

van der Pol, E., F. A. W. Coumans, A. E. Grootemaat, et al. 2014. "Particle Size Distribution of Exosomes and Microvesicles Determined by Transmission Electron Microscopy, Flow Cytometry, Nanoparticle Tracking Analysis, and Resistive Pulse Sensing." *Journal of Thrombosis and Haemostasis* 12: 1182–1192.

van der Pol, E., L. de Rond, F. A. W. Coumans, et al. 2018. "Absolute Sizing and Label-Free Identification of Extracellular Vesicles by Flow Cytometry." *Nanomedicine* 14: 801–810.

van der Pol, E., A. Sturk, T. van Leeuwen, et al. 2018. "Standardization of Extracellular Vesicle Measurements by Flow Cytometry Through Vesicle Diameter Approximation." *Journal of Thrombosis and Haemostasis* 16: 1236–1245.

van der Pol, E., M. J. C. van Gemert, A. Sturk, R. Nieuwland, and T. G. van Leeuwen. 2012. "Single vs. Swarm Detection of Microparticles and Exosomes by Flow Cytometry." *Journal of Thrombosis and Haemostasis* 10: 919–930.

van der Pol, E., T. G. van Leeuwen, and X. Yan. 2021. "Misinterpretation of Solid Sphere Equivalent Refractive Index Measurements and Smallest Detectable Diameters of Extracellular Vesicles by Flow Cytometry." *Scientific Reports* 11: 24151.

van der Pol, E., J. A. Welsh, and R. Nieuwland. 2022. "Minimum Information to Report About a Flow Cytometry Experiment on Extracellular Vesicles: Communication From the ISTH SSC Subcommittee on Vascular Biology." *Journal of Thrombosis and Haemostasis* 20: 245–251.

van Herwijnen, M. J. C., M. I. Zonneveld, S. Goerdayal, et al. 2016. "Comprehensive Proteomic Analysis of Human Milk-Derived Extracellular Vesicles Unveils a Novel Functional Proteome Distinct From Other Milk Components." *Molecular and Cellular Biology* 15: 3412–3423.

Varga, Z., Y. Yuana, A. E. Grootemaat, et al. 2014. "Towards Traceable Size Determination of Extracellular Vesicles." *Journal of Extracellular Vesicles* 3: 23298.

Vis, J. Y., and A. Huisman. 2016. "Verification and Quality Control of Routine Hematology Analyzers." *International Journal of Laboratory Hematology* 38: 100–109.

Vogt Jr. R. F., G. D. Cross, L. O. Henderson, and D. L. Phillips. 1989. "Model System Evaluating Fluorescein-Labeled Microbeads as Internal Standards to Calibrate Fluorescence Intensity on Flow Cytometers." *Cytometry* 10: 294–302.

Welsh, J. A., G. J. A. Arkesteijn, M. Bremer, et al. 2023. "A Compendium of Single Extracellular Vesicle Flow Cytometry." *Journal of Extracellular Vesicles* 12: 12299.

Welsh, J. A., D. C. I. Goberdhan, L. O'Driscoll, et al. 2024. "Minimal Information for Studies of Extracellular Vesicles (MISEV2023): From Basic to Advanced Approaches." *Journal of Extracellular Vesicles* 13: e12404.

Welsh, J. A., P. Horak, J. S. Wilkinson, et al. 2020. "FCMPASS Software Aids Extracellular Vesicle Light Scatter Standardization." *Cytometry Part A* 97: 569–581.

Welsh, J. A., J. C. Jones, and V. A. Tang. 2020. "Fluorescence and Light Scatter Calibration Allow Comparisons of Small Particle Data in Standard Units Across Different Flow Cytometry Platforms and Detector Settings." *Cytometry Part A* 97: 592–601.

Welsh, J. A., V. A. Tang, E. van der Pol, and A. Görgens. 2021. "MIFlowCyt-EV: The Next Chapter in the Reporting and Reliability of Single Extracellular Vesicle Flow Cytometry Experiments." *Cytometry Part A* 99: 365–368.

Welsh, J. A., E. van der Pol, G. J. A. Arkesteijn, et al. 2020. "MIFlowCyt-EV: A Framework for Standardized Reporting of Extracellular Vesicle Flow Cytometry Experiments." *Journal of Extracellular Vesicles* 9: 1713526.

World Health Organization. Global Health Estimates: Leading Causes of Death. https://www.who.int/data/gho/data/themes/mortality-and-global-health-estimates/ghe-leading-causes-of-death.

Yuana, Y., T. H. Oosterkamp, S. Bahatyrova, et al. 2010. "Atomic Force Microscopy: A Novel Approach to the Detection of Nanosized Blood Microparticles." *Journal of Thrombosis and Haemostasis* 8: 315–323.

Supporting Information

Additional supporting information can be found online in the Supporting Information section.

Supporting Information 1 Supporting Information 2 Supporting Information 3 Supporting Information 4 Supporting Information 5 Supporting Information 6 Supporting Information 7